Research Paper

Fabrication of Al7075-MWCNT Composite Powder by Recycling Aluminum Alloy Chips Via High Energy Milling and Alloying

Parisa Fekri Dolatabad[1], Vahid Pouyafar[2*], Ramin Meshkabadi[3]

1. Msc Student, Manufacturing Engineering Department, University of Tabriz, Tabriz, Iran
2. Assistant Professor, Manufacturing Engineering Department, University of Tabriz, Tabriz, Iran
3. Assistant Professor, Department of Engineering Sciences, Faculty of Advanced Technologies, University of Mohaghegh Ardabili, Namin, Iran

ARTICLE INFO

ABSTRACT

In this study, aluminum chips were milled in a planetary ball mill at different times and ball-to-powder weight ratios (BPRs). The resulting optimum powder was reinforced with 1 wt% and 2 wt% of multi-walled carbon nanotubes (MWCNTs). The effects of alloying time, BPR, and MWCNTs percentage on the morphology, distribution, and composition of the Al7075-MWCNT powder were investigated. The results showed that smaller particles with a limited size distribution can be obtainable by increasing BPR and decreasing mechanical milling time. A uniform dispersion of reinforcement (2 wt%) was achieved at lower alloying times (15 and 30 min) and a higher BPR (20:1). Using XRD analysis, it was revealed that the carbon peaks are more clearly in 2%-MWCNT powders than 1%-MWCNT ones. The addition of MWCNTs led to reducing the particle size; this is confirmed by the data obtained from the XRD patterns and their analysis with the Williamson-Hall model. Machining chips were converted into composite powder by cost-effective mechanical milling and alloying method with a uniform distribution of MWCNTs, which is unique.

* **Corresponding Author**
E-mail address: pouyafar@tabrizu.ac.ir

1. Introduction

Composite materials have been at the center of interest for many researchers because they are high-performance and low-cost materials. Over the last few decades, Metal Matrix Composites (MMCs) have been replaced by conventional materials in various industries [1]. The presence of several reinforcements like alumina (Al_2O_3), silicon carbide (SiC), boron carbide (B_4C), graphite (Gr), silica (SiO_2), tungsten carbide (WC), and multi wall carbon nanotubes (MWCNTs) leads to producing nanocomposites with superior mechanical properties [2-6]. Due to their unique physical, chemical, electrical and mechanical properties, MWCNTs are usually used in various scientific fields. The extraordinary strength, lightweight, and nanoscale dimensions of the MWCNTs have made them a good candidate to reinforce composites [7]. Successful preparation of ferrous [8], aluminum [9] and copper-based [10] composites with carbon-based reinforcements have been reported in recent years in terms of their preparation and application methods. However, their agglomeration and poor dispersion ability in the metal matrix make using them problematic [11]. The uniform dispersion of the MWCNTs and the MWCNT-metal interface is the most critical research topic because of dealing with the strong Van der Waals forces [12]. The production method, matrix, and type of the reinforcements determine the defectless microstructure of the MMCs and uniform distribution of particles [13]. For powder-based production methods, mechanical alloying has been widely used to decompose MWCNTs' clusters, disperse them homogeneously in the metal field, and achieve a uniform distribution [14].

The mechanical alloying properties obtained strongly depend on the mixing parameters [15]. Alloying time is one of the most influential parameters that play an essential role in the composite morphology and its mechanical properties [16]. Several studies have indicated the role of milling time to achieve a homogeneous distribution of components, which is an advantage of the mechanical milling method compared to the other conventional synthesis routes [9, 14]. In recent studies, the effect of parameters, including ball size, BPR, milling time, and speed, were studied to determine the optimal conditions of better structural, mechanical, electrical, and magnetic properties [14, 16]. Although some studies reported the improvement of mechanical properties, numerous challenges concerning the MWCNT-reinforced composites should be resolved, of which MWCNTs uniform dispersion is a significant concern. In this research, mechanical milling and alloying were used as an effective tool to disperse MWCNTs better. A high-energy planetary ball mill was employed to make Al7075-MWCNT powder. An appropriate range of the process parameters which results in a uniform dispersion should be determined. After mechanical alloying, the effect of milling time, BPR, and weight percentage of MWCNTs on the morphology of the Al7075-MWCNT powder were investigated.

2. Materials and methods

The sample in the form of machining chips with the size of 1×3 mm was utilized. The chemical composition of the chips was determined by spectrometric analysis. It includes 5.89% Zn, 2.19% Mg, 1.53% Cu, and less than a half percent of silicon, iron, manganese, titanium, chromium, and other metals. A high-energy planetary ball mill (250 rpm) was used for mechanical milling (see Figure 1). The vial and ball materials were hardened steel and chrome steel, respectively. Argon was used to prevent the chips from oxidizing during milling; in addition, 1 wt% of stearic acid was used as a process control agent (PCA) to prevent agglomeration of the particles. The chips were milled at three milling times (1, 3, and 5 h) with three different BPRs (10:1, 15:1, and 20:1).

Fig. 1. The high-energy planetary ball mill.

Mechanical alloying was utilized to better disperse the MWCNTs in the aluminum alloy. MWCNTs agglomeration changes the composite properties. Therefore, there must be an optimization process to prepare an appropriate composite powder for the alloying process. The powder chips and MWCNTs (NANOSANY CORPORATION) with an inner diameter of 5-10 nm, an outer diameter of 20-30 nm, and a length of 1-5 μm were mixed in a high-energy planetary ball mill under an argon atmosphere. The mechanical alloying conditions are as follows: 1 and 2 wt% MWCNT, three BPRs of 10:1, 15:1, and 20:1, and three alloying times of 15, 30, and 60 min. Field Emission Scanning Electron Microscopy (FESEM) model MIRA3-FEG-SEM made by TESCAN Co. (Czech Republic) was used to analyze the morphology of the powders. The size distributions of the powders were quantified using a laser particle size analyzer (FRITSCH Co., model 'ANALYSETTE 22 Nano Tec'). X-ray diffraction spectroscope (XRD) model D5000 made by Siemens was used to study intermetallic compounds. The high density of crystal defects produced by mechanical milling increases the work hardening of the powder particles. Due to severe plastic deformation and continuous fracture, the crystal dimensions are reduced to be recognizable by the X-ray diffraction peaks [17]. Williamson and Hall identified the grain size and in-lattice strain as the reason for X-ray diffraction peaks. Hence, according to Eq. (1), the grain size was determined by Williamson and Hall's method.

$$\beta \cos \theta = 4\varepsilon \sin \theta + \frac{k \lambda}{D} \qquad (1)$$

where D is the grain size, β is the peak width (in radians), θ is the angle at which the radiant beam strikes the atomic plane (in radians), ε is the relative change in distance between the crystal plates or the lattice strain, k is the Scherr constant (usually between 0.9-1), and λ is the radiated X-ray wavelength (in angstroms).

3. Results and discussion

Figure 2 shows the morphological changes of the chip after milling for 3 h with a BPR of 10:1 and 20:1. As the BPR increases, the chip morphology turns into a plate-like morphology. The sharp edges become smoother, and more welded particles became to appear. The higher the BPR, the higher the number of collisions between the balls, the powders, and the container. It leads to breaking, cold-welding, agglomerating, and again breaking the particles. These collisions speed up the milling process. In conclusion, increasing the BPR causes more chips to be broken. Figure 2 also shows the curves of the particle size distribution. D_{50} represents the minimum diameter equivalent to 50% of the particles, and D_{90}-D_{10} indicates the particle size distribution range. By increasing the BPR, D_{50} decreases from 36 μm to 6 μm, and the range of D_{90}-D_{10} encloses from 25 μm to 17 μm. Therefore, a powder with smaller particle size and a more limited distribution range is achieved.
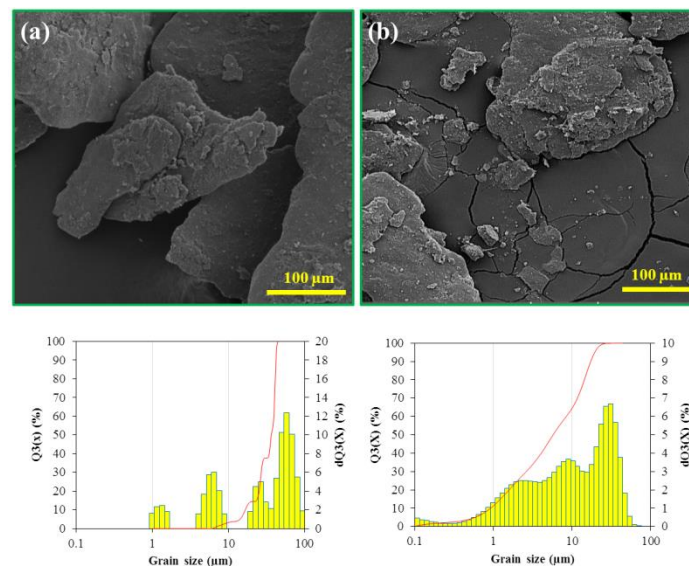
Fig. 2. The chips morphological changes and related distribution curves after milling for 3 h and a BPR of (a) 10:1 and (b) 20:1.

Figure 3 shows the morphological changes of the chip with a BPR of 15:1 after milling for 1 and 5 h. Changing the morphology of the chips in addition to agglomerating them is predicted by increasing milling time, both of which are mainly due to cold welding. At a short milling time, the particle agglomeration is not very noticeable, indicating the predominant role of the fracture and deformation process in the milling mechanism. According to the particle size distribution curves, the D_{50} increases

from 32 µm to 40 µm by increasing the milling time. It indicates that cold welding is predominant during mechanical milling. The lower D_{50} indicates the breakage of the particles. At the same time, the D_{90}-

D_{10} increases from 21 to 30 µm. Therefore, at a short milling time, the finer particles with a limited size distribution are achieved because of the priority of the fracture process compared to the cold welding.
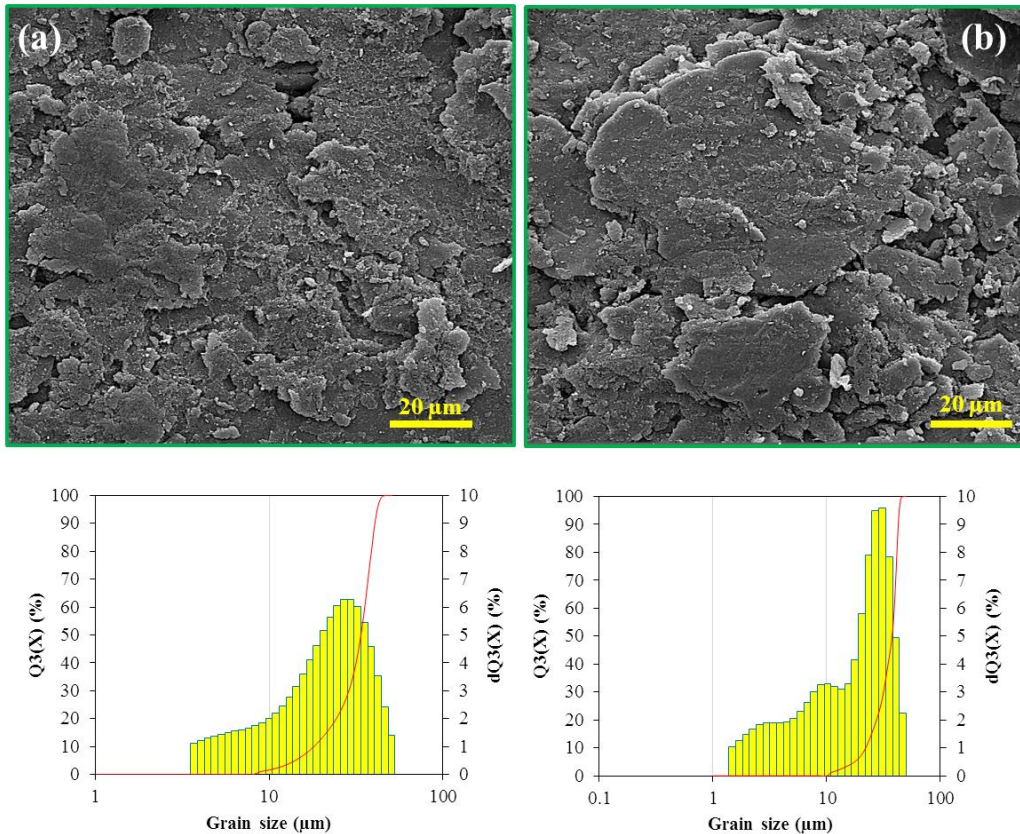
Fig. 3. The morphological changes of the chips and related distribution curves and a BPR of 15:1 after milling for (a) 1 h and (b) 5 h.

Figures 4a and b show the FESEM images of 5h-milled chips with a BPR of 10:1 and 1h-milled with a BPR of 20:1, respectively. A lower milling time with a higher BPR results in more broken chips. As the BPR increases and the milling time decreases, the D50-value decreases from 7 µm to 5.3 µm, and the particle size distribution encloses from 13.4 µm to 11.5 µm. Powders with a limited size distribution are less prone to segregation. The optimal particle size distribution can vary depending on the process conditions and the method used. There is a preference for powders with a limited size distribution over single-size or widely distributed ones due to their higher sintering potential and microstructural control [18]. These results have a good agreement with the research results conducted by Fogagnolo et al. [17].

Homogeneous distribution of the reinforcing phase in the metallic matrix is required to demonstrate the superior performance of the composite material so that the more uniform the dispersion, the better the composite properties. In this study, the alloying process and its duration determine the effective dispersion of the MWCNTs in the Al7075 alloy powder. The powder obtained from the mechanical milling for 1 h and with a BPR of 20:1 was used as an optimal combination for mechanical alloying.
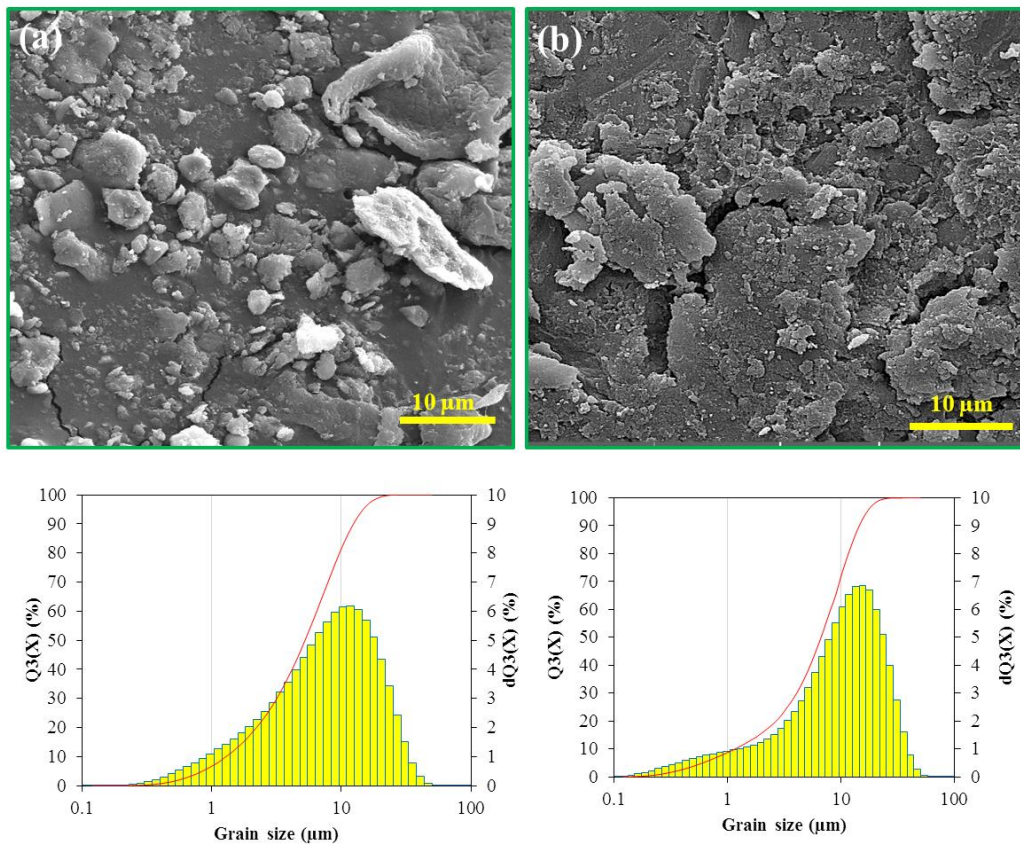
Fig. 4. The FESEM images and related distribution curves of the chips milled for (a) 5 h and a BPR of 10:1 and (b) 1 h and a BPR of 20:1.

Figure 5 shows the FESEM images of the Al7075-MWCNTs composite powders with 0, 1, and 2 wt% of reinforcing particles mechanically alloyed for 30 min with a BPR of 15:1. As we know, a mechanical mill affects particle size via two different mechanisms of cold welding and particle fracture. Figures 5a and b show that the particle size of the Al7075 containing 1wt% MWCNT composite powder is smaller than that of the Al7075 alloy powder simultaneously, i.e., the addition of the reinforcing particles reduces particle size. Furthermore, the size reduction rate is more distinguished in 2wt% MWCNT compared to 1wt% MWCNT. Therefore, it can be concluded that reinforcements have a significant impact on the morphology of the powders. The increase of the MWCNTs concentration accelerates the alloying process, causes fracture of more particles, and acts as a process control agent. The PCAs are ordinary organic compounds that act as surfactant agents. They are adsorbed onto the surface of the powder particles and minimize contact between particles, thereby inhibiting agglomeration. Here, the MWCNTs avoid cold welding and bonding between the powder particles and the balls and the agglomeration of powders during milling. So, they act as a process control agent. It also reduces cold welding during the alloying process, and smaller particles are obtained for the same alloying time. According to the results presented, adding reinforcements has a positive effect on the alloying process. The schematic of how the reinforcing particles of MWCNTs and the aluminum matrix combine in the mechanical alloying process is shown in Figure 6. Given the research results conducted by Wu et al., the particle size of the MWCNT-reinforced composite powder is smaller than the reference powder [18]. Uriza et al. [11] stated that increasing the reinforcing content is a way to reduce excessive particle welding during the milling process, which produces smaller particles at the same milling time. Increasing the MWCNT content and the collision of particles inside the mill leads to the formation of a hard surface on the particles, which increases their fragility and decreases the particle size. Therefore, in addition to the fracture-welding-fracture cycle in the mechanical milling process, this hard surface interferes with the cycle and becomes harder each time during combination with the aluminum particles. As the MWCNT content increases, this effect reaches a maximum value, and the fracture of the harder and smaller particles prevails. Figure 6 illustrates the mechanical alloying mechanism of the Al7075-MWCNT composite.
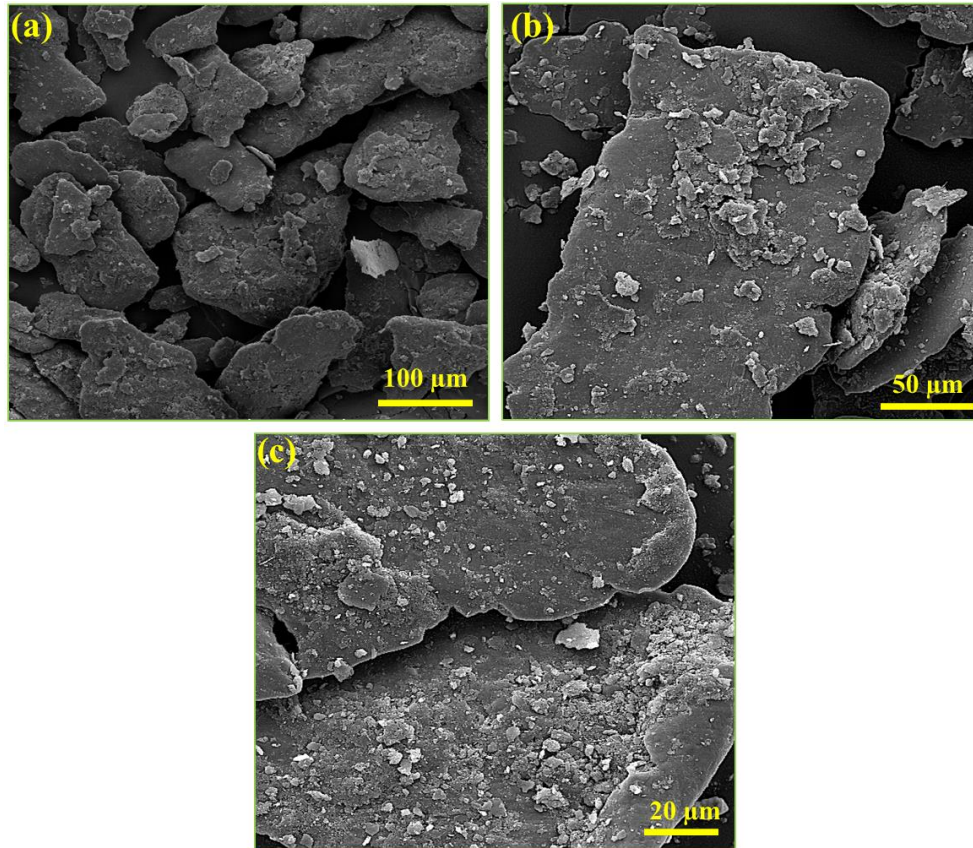
Fig. 5. The FESEM images of the Al7075-MWCNTs composite powders with (a) 0, (b) 1, and (c) 2 wt% reinforcement mechanically alloyed for 30 min and a BPR of 15:1.
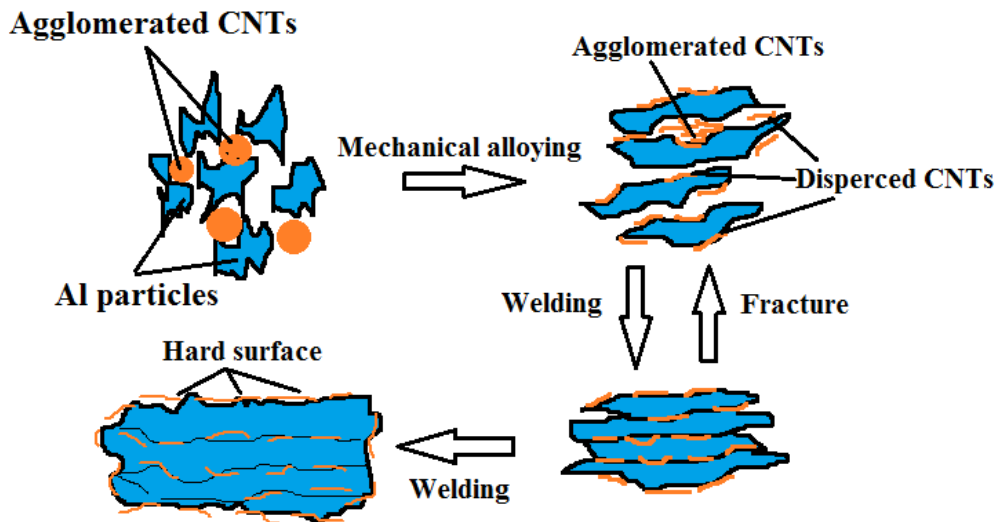
Fig. 6. Schematic of mechanical alloying mechanism of Al7075-MWCNT composite.

Figure 7 presents the FESEM images of Al7075-MWCNTs composite powder after alloying for 60 min and a BPR of 10:1. Figure 7a shows the morphology of a composite powder with 1 wt%-MWCNTs. A plate-to-globular change in the morphology of the particles and more fracture of particles are observable after mechanical alloying. MWCNTs were distributed in the matrix so that some of them are deeply embedded inside the alloy, and partial clusters are seen. By increasing the reinforcements up to 2 wt% (see Figure 7b), the MWCNTs observed on the composite surface gradually decrease and embed inside the aluminum alloy particles. The morphology of clusters of the MWCNTs is not changed.
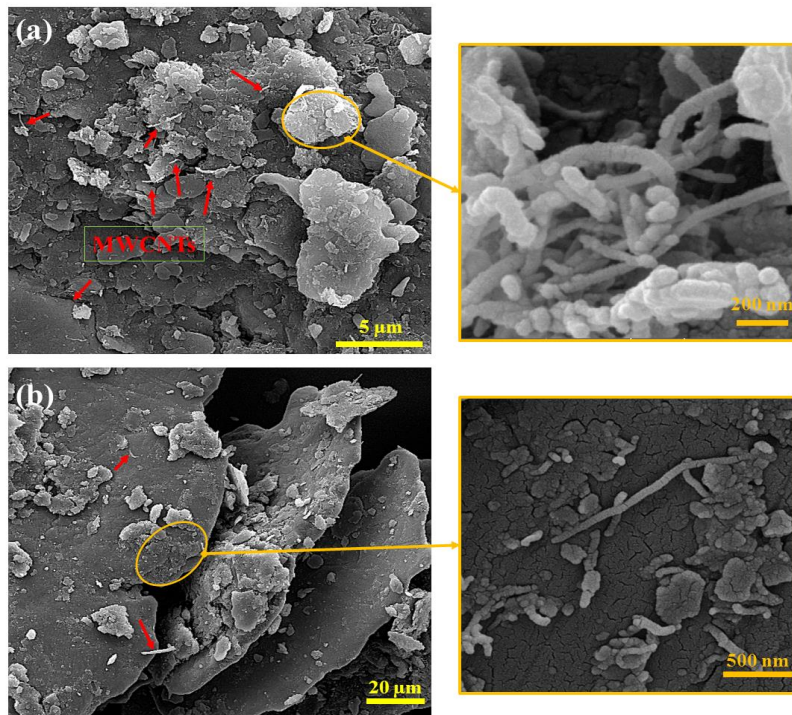
Fig. 7. The FESEM images of the Al7075-MWCNT composite powder mechanically alloyed for 60 min, a BPR of 10:1, and a reinforcement content of (a) 1% and (b) 2%.

Figure 8 shows the FESEM images of the Al7075-MWCNTs composite powder after an alloying time of 15 min and a BPR of 20:1. Based on Figure 8a, the MWCNTs are rarely found on the surface; this is attributable to the lower percentage of reinforcements or the higher BPR at a short alloying time. This condition leads to uniformly dispersing and deeply embedding the MWCNTs inside the alloy. Of course, by increasing the BPR during the mechanical alloying process, some breakage is observed in the MWCNTs due to the higher energy of the planetary ball mill. Figure 8b shows the uniform distribution of the MWCNTs on the surface of the composite powder in which their clusters are crushed and bonded to the surface of the aluminum particles. It is evident that uniform dispersion of reinforcements is achieved by increasing their content in a short alloying time.
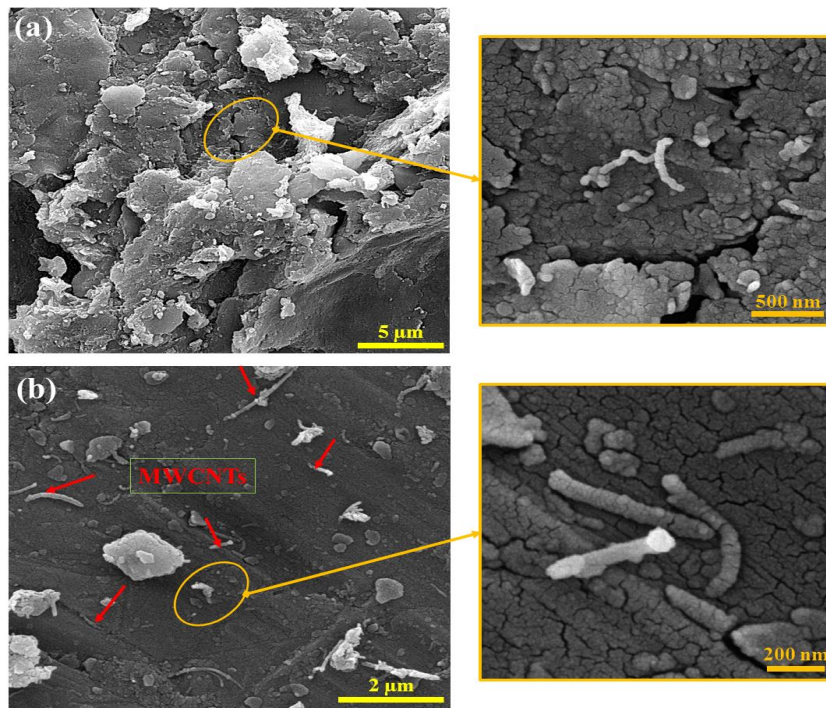
Fig. 8. The FESEM images of the Al7075-MWCNT composite powder mechanically alloyed for 15 min, a BPR of 20:1, and a reinforcement content of (a) 1% and (b) 2%.

Figure 9 presents the FESEM images of the Al7075-2%-MWCNTs composite powder with a BPR of 10:1 and an alloying time of 15 min. It can be seen that in MWCNTs-rich composite powder made with a low BPR and alloying time, the accumulation of nanotubes on the particle surface prevents the metal particles from bonding to each other. In this case, two types of bonds (1) Al7075 alloy with MWCNTs and (2) MWCNTs with MWCNTs are formed. The bond between the nanotubes is fragile and breakable under the load applied [19]. Further accumulation of the MWCNTs in a short alloying time leads to agglomerating the particles and adversely affects the homogeneity of the composite powders [20, 21]. In other investigations, the mechanical alloying process has successfully dispersed MWCNTs [19, 20]. In the research conducted by Al-Aqeeli [20], Yarahmadii et al. [19], increasing the content of reinforcements results in agglomeration when the milling time is short. In order to study the formation of the composite and the distribution of the reinforcement phase, EDS-map was prepared from Al7075-2% MWCNT powder with a BPR of 10:1 and alloying time of 15 minutes which is shown in Figure 9. To better understand the distribution of the reinforcements, a carbon element map was prepared as a representative of the MWCNT phase. It is observed that the carbon element is dispersed in the aluminum background, and a composite powder is formed.
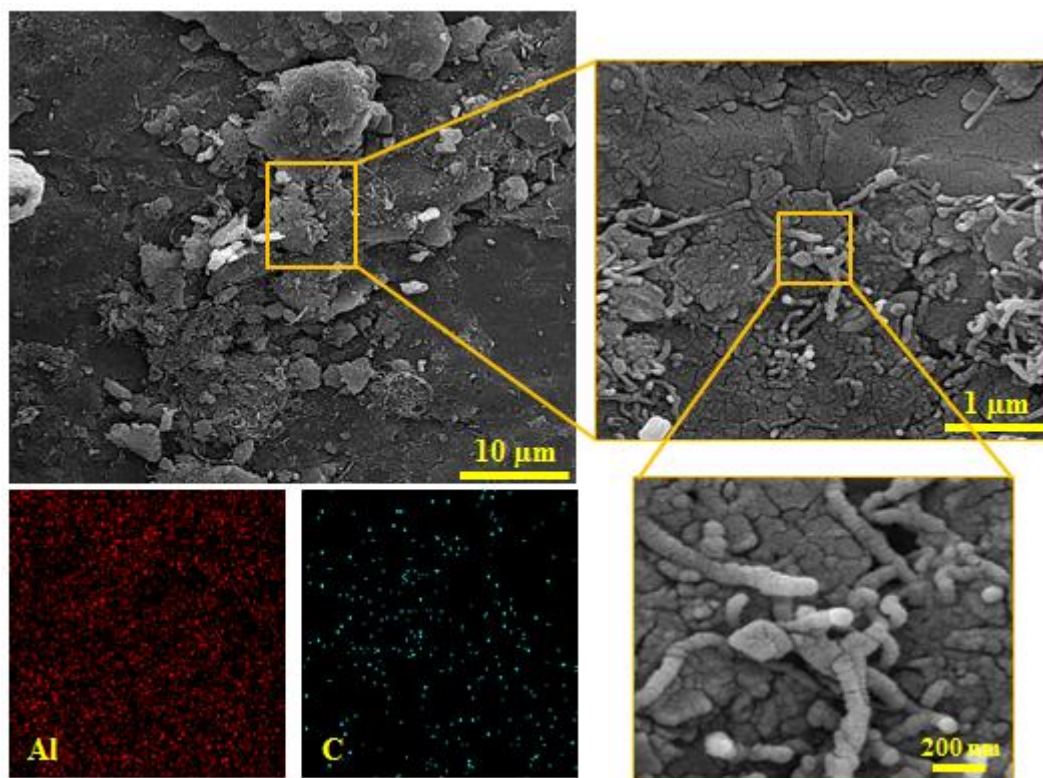
Fig. 9. The FESEM images of the Al7075-2% MWCNTs composite powder with a BPR of 10:1 and an alloying time of 15 min along with the EDS-map

Figure 10 shows the X-ray diffraction (XRD) spectroscopy analysis results for Al7075 alloy with 0, 1, and 2 wt% reinforcement. According to Figure 10b, the carbon-related peaks are tiny due to the low content of MWCNTs (1%), but these peaks can be seen by increasing the percentage of the MWCNTs, as shown in Figure 10c. Due to the large amount of Mg and Zn elements in the Al7075 alloy and the strong tendency of the alloy to combine with these elements, MgZn created during the alloying process is observed among all phases. In a study conducted by Zhang et al. [22], $MgZn_2$ was also observed during a tempering process in the hot pressing process of the Al7075 alloy. The difference in the thermal expansion coefficients between the MWCNTs and the background Al7075 alloy increases the deposition of $MgZn_2$ and the bonds between the MWCNTs and aluminum. The $MgZn_2$ phase has a good relationship with the aluminum matrix and helps to increase the surface bond. It should be noted that in Figs. 10b and c, the purpose is to show the appearance of the carbon peaks, and the peaks corresponding to the Al and MgZn phases are not shown for better comparison.
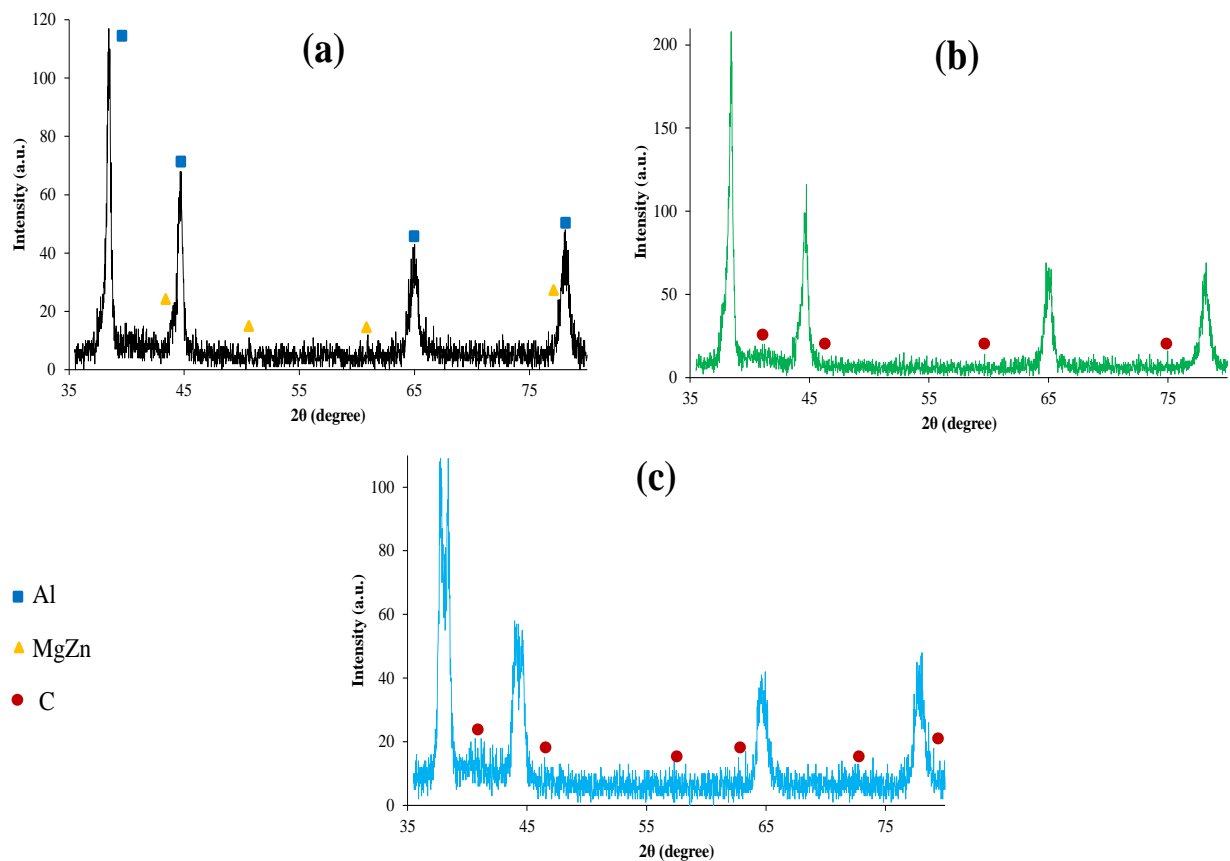
Fig. 10. The XRD analysis of the Al7075-MWCNT powder containing (a) 0, (b) 1, and (c) 2 wt% reinforcement (alloying time: 60 min, BPR: 10:1).

The morphological changes influence the intensity and width of the X-ray diffraction peaks. For example, when the grain size decreases, the width of the peak increases while its intensity decreases. Moreover, the intensity of some peaks increases and some others decreases by the preferential orientation of the grains. Using the data extracted from the XRD pattern and Xpert High Score software, the $\beta cos\theta$ diagram was plotted in terms of $sin\theta$ as shown in Figure 11a. According to the Williamson-Hall model, the grain size is calculated by the width obtained from the line's origin. The grain size is extracted from the intersection of the graph with the Y-axis shown in Figure 11a. Based on the results shown in Figure 11b, the grain size is reduced by adding the reinforcements to the Al7075 alloy. After alloying for 60 min, the grain size of the Al7075 alloy with 0, 1, and 2 wt% MWCNTs are equal to 37.4, 32.2, and 29.4 nm, respectively. By comparing the X-ray diffraction pattern of these samples, it is clear that by increasing MWCNTs, the peaks of the reinforcements become wider and have a larger peak width, indicating a decrease in the grain size. Compared to the Al7075 alloy powder without the reinforcements, the grain size of the Al7075 containing 2wt% MWCNTs powders at the same alloying time and BPR are reduced by about 22%. Therefore, based on the results obtained from the FESEM images, the reinforcements as a process agent accelerate the alloying process and reduce the grain size.

(a)

(b)
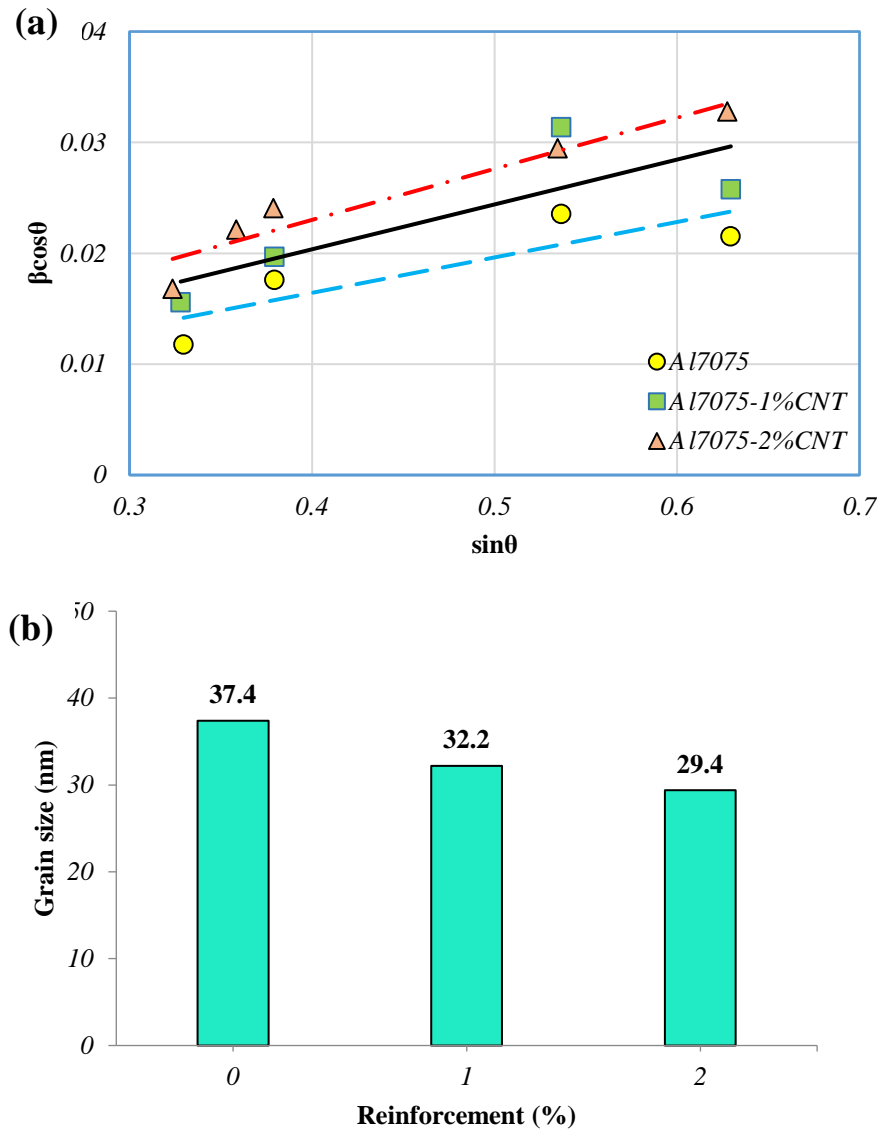
Fig. 11. (a) The Williamson-Hall diagram and (b) the obtained grain size (alloying time: 60 min, BPR: 10:1).

4. Conclusions

In this research, the Al7075-MWCNT composite powder was prepared by the mechanical alloying process in a high-energy planetary ball mill with different weight percentages of reinforcements, milling time, and BPR. The composites morphology was studied, and the following results were obtained:

• In mechanical milling, by decreasing the milling time in a constant BPR, the finer particles with a limited size distribution are achieved because of the priority of the fracture process compared to the cold welding one. As the BPR increases and the milling time decreases simultaneously, the powders with a limited size distribution are achieved.

• In the mechanical alloying process, the reinforcements had a significant impact on the morphology of the powders. By increasing the

MWCNTs, the formation of harder surfaces on the particles accelerates; it should be mentioned that their fragility increases, the cold welding decreases, and smaller particles are obtained.

• A uniform dispersion of the reinforcement (2 wt%) inside the metallic background of the Al7075 alloy is achieved after alloying for 15 and 30 min and a BPR of 20:1. In addition, adding a large amount of the MWCNTs (2 wt%) at a short alloying time (15 min) and a lower BPR (10:1) adversely affect the homogeneity of the alloy and leads to agglomeration.

• There is no new peak in the XRD diffraction pattern for the Al7075 aluminum alloy powder. In the X-ray diffraction pattern of the Al7075 containing 1 wt% MWCNT, the carbon peaks are specified in small quantities. For Al7075 containing 2 wt% MWCNT, the carbon peak is more visible compared

to the 1 wt% MWCNT. The MgZn phase peaks are also evident in the X-ray diffraction patterns; this is due to the combination of the Mg and Zn elements present in the Al7075 alloy during the alloying process.

• The result concerning the reduced particle size, which is due to the addition of the MWCNTs, is confirmed based on the data obtained from the XRD pattern and their analysis with the Williamson-Hall model.

References

[1] Samal P., Vundavilli P.R., Meher A., Mahapatra M.M., 2020, "Recent progress in aluminum metal matrix composites: A review on processing, mechanical and wear properties," J Manuf Process, 59, pp. 131-152.

[2] Prajapati P., Chaira D., 2019, "Fabrication and characterization of Cu–B4C Metal matrix composite by powder metallurgy: effect of B 4 C on Microstructure, mechanical properties and electrical conductivity," Trans Indian Inst Met, 72(3), pp. 673-684.

[3] Bakkar S., Wall M., Ku N., Berman D., Aouadi S.M., Brennan R.E., et al., 2021, "Al/Al$_2$O$_3$ metal matrix composites produced using magnetic field-assisted freeze-casting of porous ceramic structures," J Mater Res, 36(10), pp. 2094-2106.

[4] Ashwath P., Xavior M.A., 2016, "Processing methods and property evaluation of Al$_2$O$_3$ and SiC reinforced metal matrix composites based on aluminium 2xxx alloys," J Mater Res, 31(9), pp. 1201-1219.

[5] shafqat Q.A., Rafi ud d., Shahzad M., Khan M., Mehmood S., Syed W.A., et al., 2019, "Mechanical, tribological, and electrochemical behavior of hybrid aluminum matrix composite containing boron carbide (B$_4$C) and graphene nanoplatelets," J Mater Res, 34(18), pp. 3116-3129.

[6] Liu G., Tao J., Li F., Bao R., Liu Y., Li C., et al., 2019, "Optimizing the interface bonding in Cu matrix composites by using functionalized carbon nanotubes and cold rolling," J Mater Res, 34(15), pp. 2600-2608.

[7] Kumar A., Banerjee U., Chowrasia M.K., Shekhar H., Banerjee M., 2019, "Effect of MWCNT Content on the structure and properties of spark plasma-sintered Iron-MWCNT composites synthesized by high-energy ball milling," J Mater Eng Perform, 28(5), pp. 2983-3000.

[8] Polat G., Canbolat I.E., Uzunoğlu A., Kotan H., 2021, "Effect of milling time, MWCNT content, and annealing temperature on microstructure and hardness of Fe/MWCNT nanocomposites synthesized by high-energy ball milling," Adv Powder Technol, 32(8), pp. 3107-3116.

[9] Bastwros M., Kim G.-Y., Zhu C., Zhang K., Wang S., Tang X., et al., 2014, "Effect of ball milling on graphene reinforced Al6061 composite fabricated by semi-solid sintering," Composites, Part B, 60(pp. 111-118.

[10] Shu R., Jiang X., Shao Z., Sun D., Zhu D., Luo Z., 2019, "Fabrication and mechanical properties of MWCNTs and graphene synergetically reinforced Cu–graphite matrix composites," Powder Technol, 349(pp. 59-69.

[11] Uriza-Vega E., Carreño-Gallardo C., López-Meléndez C., Cuadros-Lugo E., Pérez-Bustamante R., Ledezma-Sillas E., et al., 2019, "Mechanical Behavior of Multiwalled Carbon Nanotube Reinforced 7075 Aluminum Alloy Composites Prepared by Mechanical Milling and Hot Extrusion," Mater Res, 22(2), pp.

[12] Chen B., Kondoh K., Imai H., Umeda J., 2016, "Effect of initial state on dispersion evolution of carbon nanotubes in aluminium matrix composites during a high-energy ball milling process," Powder Metall, 59(3), pp. 216-222.

[13] Singh N., Shadangi Y., Goud G.S., Pandey V.K., Shivam V., Mukhopadhyay N.K., 2021, "Fabrication of MgAlSiCrFe Low-Density High-Entropy Alloy by Mechanical Alloying and Spark Plasma Sintering," Trans Indian Inst Met, pp.

[14] Aslibeiki B., Kameli P., 2020, "Structural and magnetic properties of Co/Al$_2$O$_3$ cermet synthesized by mechanical ball milling," Ceram Int, 46(12), pp. 20116-20121.

[15] Azimi A., Shokuhfar A., Nejadseyfi O., 2015, "Mechanically alloyed Al7075–TiC nanocomposite: Powder processing, consolidation and mechanical strength," Mater Des, 66(pp. 137-141.

[16] Wagih A., Fathy A., Kabeel A., 2018, "Optimum milling parameters for production of highly uniform metal-matrix nanocomposites with improved mechanical properties," Adv Powder Technol, 29(10), pp. 2527-2537.

[17] Fogagnolo J., Velasco F., Robert M., Torralba J., 2003, "Effect of mechanical alloying on the morphology, microstructure and properties of aluminium matrix composite powders," Mater Sci Eng, A, 342(1-2), pp. 131-143.

[18] Wu Y., Kim G.-Y., Russell A.M., 2012, "Effects of mechanical alloying on an Al6061–CNT composite fabricated by semi-solid powder processing," Mater Sci Eng, A, 538(pp. 164-172.

[19] Yarahmadii A., Rajabi M., Talafi Noghani M., Taghiabadi R., 2019, "Synthesis of aluminum-CNTs composites using double-pressing double-sintering method (DPDS)," J Nanostruct, 9(1), pp. 94-102.

[20] Al-Aqeeli N., 2013, "Processing of CNTs reinforced Al-based nanocomposites using different consolidation techniques," J Nanomater, 2013(pp.

[21] Wu Y., Kim G.-Y., Russell A.M., 2012, "Mechanical alloying of carbon nanotube and Al6061 powder for metal matrix composites," Mater Sci Eng, A, 532(pp. 558-566.

[22] Zhang H., Wang B., Zhang Y., Li Y., He J., Zhang Y., 2020, "Influence of aging treatment on the microstructure and mechanical properties of CNTs/7075 Al composites," J Alloys Compd, 814(pp. 152357.